

Archie's "n" Exponent: *The rest of the story*

Gene Ballay and Nelson Suarez
www.GeoNeurale.com

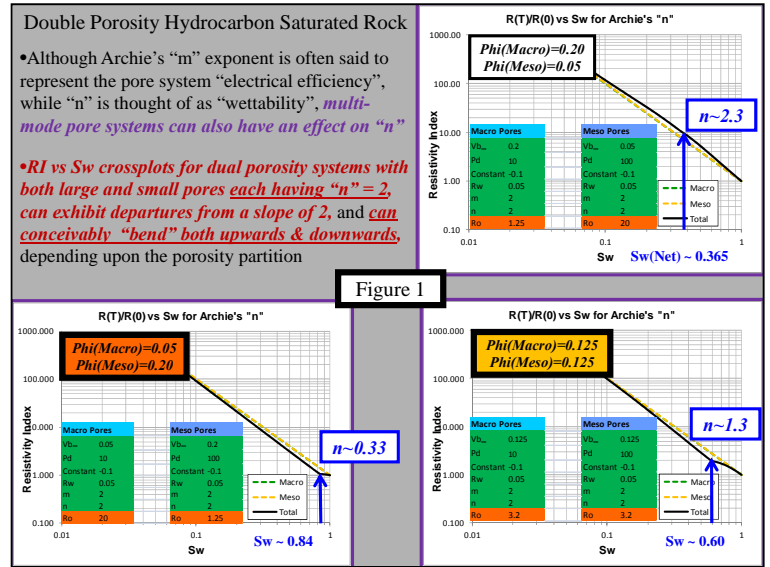
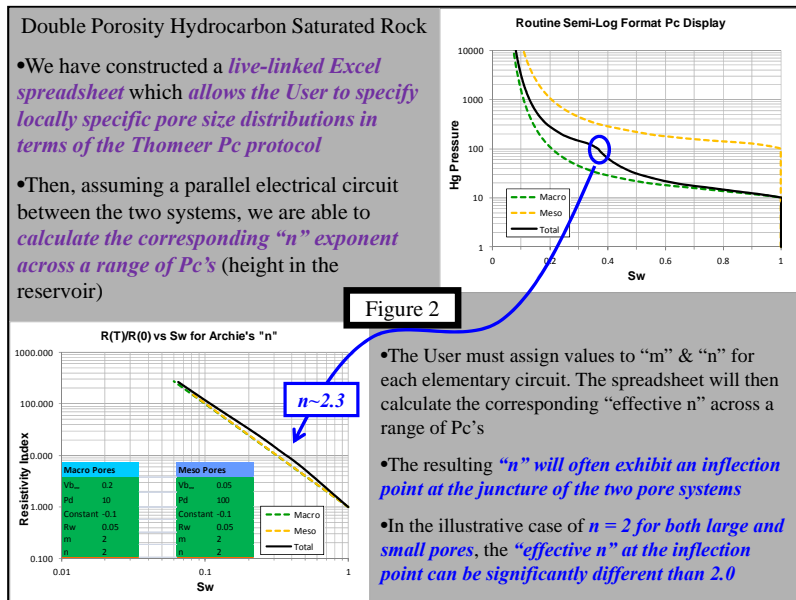
In an earlier note (The "m" Exponent in Carbonate Petrophysics) we discussed the physical meaning and range of values of Archie's "m" exponent; here we move on to the "n" exponent.

Conceptually the **Cementation Exponent** represents the "efficiency" of a brine saturated pore system to conduct electricity relative to the conductivity of the brine itself. The **Saturation Exponent** describes the "efficiency" of a partially brine saturated pore system to conduct electricity in the presence of a non-conductive hydrocarbon phase, relative to the fully brine saturated baseline.

We then mentally realize that "n" will be related to wettability. Should the rock take on an oil-wet character, the conductive brine phase will begin to be "choked off" somewhat analogous to the cemented bead pack effects on "m", investigated by Wyllie and Gregory.

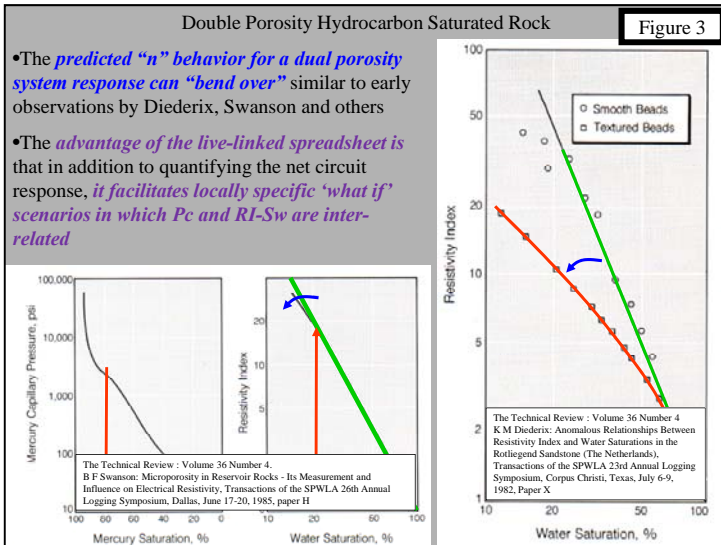
What may be *less immediately obvious is the role that the basic pore system can play in "n"*. In many cases, the essence of carbonate petrophysics relative to clastic petrophysics is that of pore system heterogeneity versus clay conductivity. And *should there be a multi-mode pore system, there may well be an effect on both "m" and "n": Figure 1.*

In the case of a single-mode pore system, we often find a linear relation (on a Log-Log display)



between the Resistivity Index [R(Sw<100%)/R(Sw=100%)] and Sw across a large range of saturations, with a single slope that is related to Archie's exponent "n". **Multi-mode pore systems can result in a non-linear relation** (multiple & different slopes) **between the RI and Sw, independent of the wettability, giving rise to what is termed non-Archie behavior: Figure 2.**

Emmanuel Toumelin & Carlos Torres-Verdin, Bernard Montaron, Marc Fleury and others have investigated this issue in some detail. **Our objective herein is to illustrate the issue with basic circuit**



theory and to develop a dynamic Pc-referenced spreadsheet that allows one to perform “what if” calculations for locally specific conditions.

The **“bending over” of the RI – Sw crossplot, at the saturation corresponding to the capillary displacement pressure of the second pore system has been observed in both bead pack and reservoir rock studies: Figure 3.**

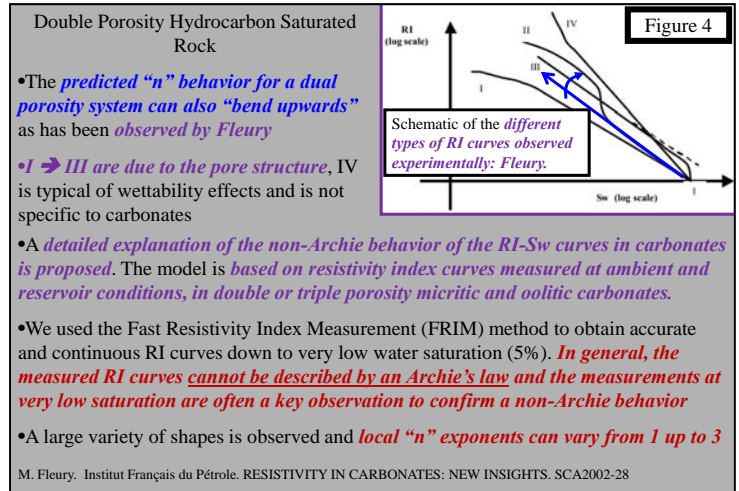
As if one non-intuitive response were not enough, we find that **the RI-Sw trend of dual porosity rock can also “bend upwards”**

and again the inflection point is related to the porosity partition: Figure 4.

It is important to realize that while the parallel circuit model used herein is common in the literature and does illustrate how the “n” exponent is affected by the pore system, not all reservoir rock will be configured as such. Complications beyond what these calculations assume include an electrical circuit that is not strictly parallel and variations in wettability (certainly possible when there is a range of pore sizes).

Archie’s Exponents

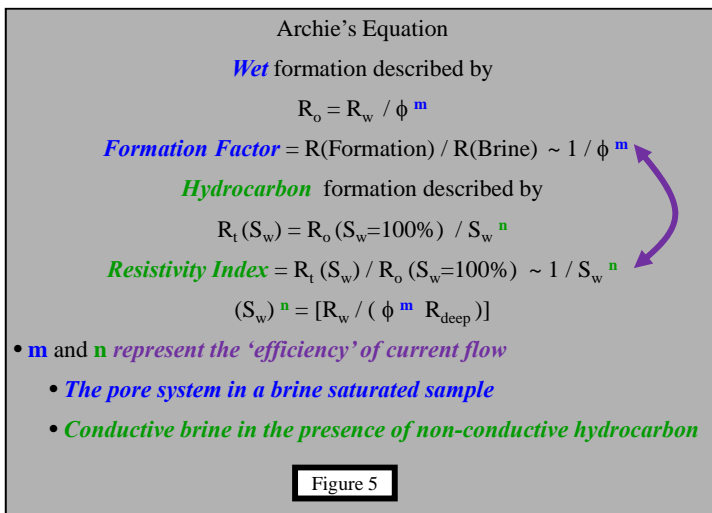
As we all know, Archie performed a series of ground-breaking measurements that, when combined with the follow-up work of others, now forms the basis of our usual formation



evaluation algorithms: **Figure 5.**

Schlumberger’s Technical Review, Volume 36 Number 3 and Volume 36 Number 4 provide a nice chronologically ordered technical discussion of the Formation Factor (“m” exponent) and Resistivity Index (“n” exponent). We have discussed the “m” exponent in an earlier note, and here focus on “n”.

Given that **“n” represents the “efficiency” of current flow through a conductive brine phase in the presence of a non-conductive hydrocarbon phase, the first issue that comes**



to mind is wettability: Figure 6.


Should the reservoir rock take on an oil-wet character, the electrical “efficiency” will be reduced, requiring a mathematical increase in “n” for proper representation. Although the concept is simple to visualize, practical implementation can be challenging, since the wettability may be a function of Height (Another Look at Ekofisk Wettability by G. Hamon.).

Archie’s “n” Exponent : Wettability


- **Wettability** will have an obvious influence on “n”
- Current flow in an **oil wet rock is less ‘efficient’, more tortuous**
- **‘n’ will be higher**

Figure 6

Water Wet



Oil Wet



The Technical Review : Volume 36 Number 4

Furthermore, should there be a dual porosity system the larger pore throats will have the

opportunity to become oil wet at a deeper depth than will the small pore throats (Middle East Well Evaluation Review: No 17, 1996).

Perhaps **less obvious as having an influence on “n” is the presence of a rough grain surface**. When Diederix reviewed his RI – Sw measurements, he noticed that while many were linear (as expected), some exhibited an inflection point: **Figure 7**.

When the samples were examined by SEM, he further observed that **those**

Archie’s “n” Exponent : Multiple Pore Systems

- **Diederix** investigated **Grain Surface Effects**
- He **observed ‘inflection points’** in some (but not all) of his resistivity index measurements
 - SEM revealed the **‘inflection point’** correlated with the **presence of a rough grain surface**
 - Samples with **smooth grain surfaces** had no ‘knee’
- **Diederix theorized** that the **rough surface would ‘hold’ water more efficiently** (as compared to a smooth surface)
 - **Offer a more conductive current path : lower “n”**
 - This is a **surface effect, not a clay conductivity, issue**

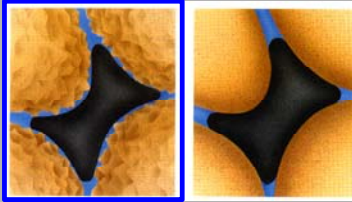


Figure 7

The Technical Review : Volume 36 Number 4
K M Diederix: Anomalous Relationships Between Resistivity Index and Water Saturations in the Rotliegend Sandstone (The Netherlands), Transactions of the SPWLA 23rd Annual Logging Symposium, Corpus Christi, Texas, July 6-9, 1982, Paper X

exhibiting an inflection point had rough surfaces whereas the (expected) linear response corresponded to smooth surface grains, and this caused him to speculate that the rough surfaces might be providing a second electrical circuit.

Diederix followed up with a **bead pack study** in which **RI – Sw was measured on two water-wet packs: one set of beads had smooth surfaces while the second set had rough surfaces**.

The rough surface beads exhibited a non-linear RI – Sw relation while the smooth surface beads remained linear (but eventually bent over, as even a

Archie’s “n” Exponent : Multiple Pore Systems

- **Diederix simulated** grain roughness effects **in the lab**
- **Smooth and rough glass beads**
 - **Both bead packs water wet**
 - **No inflection point** observed in **smooth surface beads**
 - **Rough surface bead packs** exhibited **‘inflection point’** just as the rough reservoir rock did
- **Rough grain surface** leads to **lower saturation exponent**

The Technical Review : Volume 36 Number 4
K M Diederix: Anomalous Relationships Between Resistivity Index and Water Saturations in the Rotliegend Sandstone (The Netherlands), Transactions of the SPWLA 23rd Annual Logging Symposium, Corpus Christi, Texas, July 6-9, 1982, Paper X

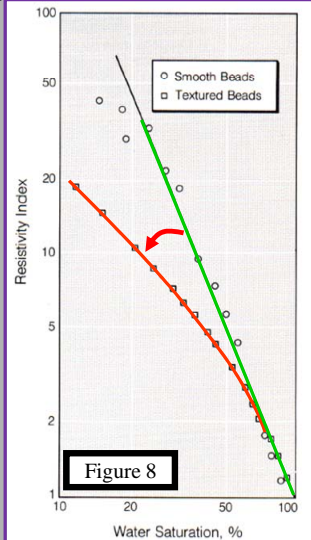


Figure 8

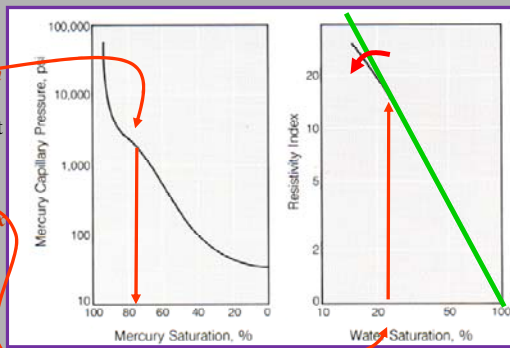
Archie's "n" Exponent : Multiple Pore Systems

•Swanson investigated dual porosity *in the lab*

•He found the *RI - Sw trend consistently changed slope* at the saturation *where Pc curve indicated a transition from* (large) *inter-granular to* (small) *micro-porosity*

Figure 9

- Left: *Micropores begin to contribute* to 'rock' response at *~ 2000 psi*, at which point *the water saturation is ~ 25 %*
- Right: *Resistivity Index 'bends over'* as the micropores come into play at *~ 25 su*



The Technical Review : Volume 36 Number 4
B F Swanson: Microporosity in Reservoir Rocks - Its Measurement and Influence on Electrical Resistivity, Transactions of the SPWLA 26th Annual Logging Symposium, Dallas, June 17-20, 1985, paper H

smooth surface becomes rough at some dimension): **Figure 8**.

Bearing in mind that both bead packs were water wet, **these results indicated that an attribute in addition to wettability was influencing "n"**.

Diederix was followed by Swanson who both mathematically modeled, and experimentally measured, the Pc and RI-Sw properties of dual porosity samples: **Figure 9**.

Swanson found that the RI-Sw plot "bent over" at the Sw corresponding to entry of hydrocarbon into the smaller pores.

In the time since Swanson, a number of additional investigations have been performed, with increasingly sophisticated mathematical models. **Our objective herein is to establish the basic concept, and to further construct a live-linked Pc ⇔ RI-Sw spreadsheet which will (simply) illustrate the effect of a dual porosity system on the "n" exponent for locally specified conditions.**

Basic Circuit Theory

The Pc curve, as specified by the User, will define the brine saturation in the two pore systems, as a function of pressure (height in the reservoir). At the simplest level, the two pore systems may exist in a parallel or series arrangement, with the parallel configuration being the analogue of a dispersed shaly sand model (Waxman-Smits, for example).

We all realize that Mother Nature is not likely to take on the most mathematically convenient configuration, but we must "walk before we can run" and furthermore the current objective is only to achieve a first pass illustration and calculation.

The **current flow is described with an Ohm's Law parallel circuit: Figure 10**.

In the case of a parallel circuit, the voltage drop across the various elements is identical, and equal to $I * R$. The total current through the circuit is the sum of that passing through the

Ohm's Law and Circuit Models

- Ohm's Law for DC current flow is $V = I * R$
 - V → voltage, I → Current, R → Resistance
- In a *parallel circuit, the various elements each experience the same voltage drop, V*
- The *net current through the circuit is*
 - $I = I(1) + I(2) + \dots + I(n)$, where the i^{th} element satisfies $I(i) = V(i) / R(i)$
 - $I = V * [1/R(1) + 1/R(2) + \dots + 1/R(n)]$
 - $C = 1 / R$
 - $I = V * C = V * [1/R(1) + 1/R(2) + \dots + 1/R(n)] = V * [C(1) + C(2) + \dots + C(n)]$
- Ohm's Law for the entire circuit is then
 - $V = I / C = I / [1/R(1) + 1/R(2) + \dots + 1/R(n)] = I / [C(1) + C(2) + \dots + C(n)]$
- The *'effective' parallel circuit conductivity is the sum of the separate conductivities.*
- In the case of a two component circuit, $C(\text{eff}) = C(1) + C(2)$

Figure 10

http://en.wikipedia.org/wiki/Parallel_circuit

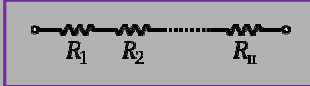
various elements, which with a bit of algebra, brings us to the observation that the effective conductivity (inverse of resistivity) is the sum of the individual conductivities.

Although our focus is on a parallel circuit, this is a convenient point at which to determine the response characteristic of a series circuit, in case that configuration should be referenced at a later time. Now the total voltage drop across the entire circuit is the sum of the individual voltage drops, while the current flow through each element is identical: **Figure 11**.

In the case of a series arrangement, we then find that the effective resistivity is the sum of the individual resistivities.

Ohm's Law and Circuit Models

• In a *series circuit*, the various elements each experience the same current flow, I



• The *net voltage across the circuit* is

- $V = V(1) + V(2) + \dots + V(n)$, where the i^{th} element satisfies $V(i) = I * R(i)$

• Ohm's Law *for the entire circuit* is then

- $V = I * R(1) + I * R(2) + \dots + I * R(n) = I * [R(1) + R(2) + \dots + R(n)]$

• The '*effective*' *series circuit resistivity* is the sum of the separate resistivities.

• If the equation is written *in terms of conductivity*, we have

- $V = I / C = I * [1/C(1) + 1/C(2) + \dots + 1/C(n)]$
- $1 / C = 1/C(1) + 1/C(2) + \dots + 1/C(n)$

• The '*effective*' *series circuit conductivity* is inversely related to the sum of the individual inverse conductivities.

• In the case of a *two component circuit*, $1/C(\text{eff}) = 1/C(1) + 1/C(2)$

http://en.wikipedia.org/wiki/Parallel_circuit

Figure 11

The Thomeer Capillary Pressure Model

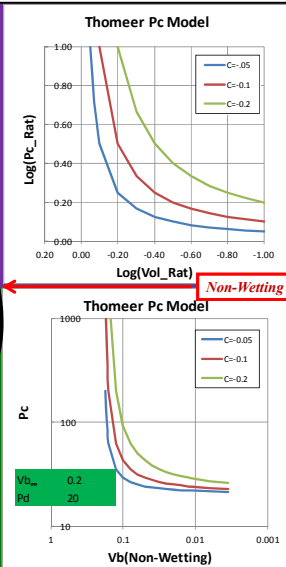
The Thomeer Capillary Pressure Model

- The *Thomeer capillary pressure model* is a *hyperbolic relation between Mercury Injection Pressure (Pc) and Bulk Volume (Vb) Occupied* (by the non-wetting mercury), expressed as follows
- $[\text{Log}(Vb / Vb_{\infty})] [\text{Log}(Pc / Pd)] = \text{Constant}$
- Vb_{∞} is the *fractional bulk volume occupied by mercury extrapolated to infinite mercury pressure*
- P_d is the *extrapolated mercury displacement pressure*
- *Constant* is related to the *pore geometric factor* and reflects the distribution of pore throats and their associated volumes: *the curvature of the relation*
- In general we desire a *direct Pc ⇔ Vb relation*, which is *achieved by raising each side of the equation to the power 10*,

$Vb/Vb_{\infty} = 10^{[\text{Constant}/(\text{Log}(Pc/Pd))]}$

George Hirasaki. Hydrostatic Fluid Distribution. www.owl.net.rice.edu/~ceng671/CHAP3.pdf

Figure 12



Hyperbolic models appear in a variety of petrophysical discussions, with one common application being **Bulk Volume Water**: $BVW = \Phi * S_w$. Above the transition zone, BVW takes on a relatively constant value for a specific rock quality, and rock of a specific category (BVW) can be often be safely (minimal risk of producing water) perforated in the presence of high S_w , so long it falls along the appropriate BVW trend (Ross Crain, 2009).

The **Thomeer model of capillary pressure is a hyperbolic relation between Mercury Injection Pressure (Pc) and Bulk Volume (Vb) Occupied** [by the non-wetting mercury, or vice versa ($1 - S_{at,wetting}$)], expressed as follows: **Figure 12**.

The **Thomeer model of capillary pressure is a hyperbolic relation between Mercury Injection Pressure (Pc) and Bulk Volume (Vb) Occupied** [by the non-wetting mercury, or vice versa ($1 - S_{at,wetting}$)], expressed as follows: **Figure 12**.

Volume (Vb) Occupied [by the non-wetting mercury, or vice versa ($1 - S_{at,wetting}$)], expressed as follows: **Figure 12**.

$$[\text{Log}(Vb / Vb_{\infty})] [\text{Log}(Pc / Pd)] = \text{Constant}$$

- Vb_{∞} is the **vertical asymptote**: the total interconnected volume accessible by the mercury (Hirasaki)
- P_d is the horizontal asymptote: the **extrapolated mercury displacement pressure** in psi, the pressure required to enter the largest pore throat.

- **Constant** is the **pore geometry factor**, related to the distribution of pore throats and their associated volumes: the curvature of the relation.

The Thomeer Capillary Pressure Model

•The 10^x term is often converted to e^y so that Thomeer's final expression involves both Base 10 and Base e logarithms

$$\frac{(V_b)_{P_c}}{(V_b)_{P_\infty}} = e^{-G/\text{Log}(P_c/P_d)}$$

• $(V_b)P_\infty$ is the **fractional bulk volume occupied by mercury extrapolated to infinite mercury pressure**

• P_d is the **extrapolated mercury displacement pressure** in psi

• G is the **pore geometric factor**, reflecting the distribution of pore throats and their associated volumes and **related to the Hyperbolic Constant** as

$$G = -0.4343 * \text{Hyperbolic Constant}$$

George Hirasaki. Hydrostatic Fluid Distribution. www.owlnet.rice.edu/~ceng671/CHAP3.pdf

Log-Log plot for fitting Hg/air Pc data with Thomeer model

Figure 13

Thomeer's protocol is useful for both constructing physically realistic, generic Pc curves, and for curve-fitting measured data. In the case of performing a curve fit to independently measured data, we expect V_b_∞ to be about equal to the sample porosity for high permeability rock, but possibly somewhat different in lower quality rock: **Figure 13.**

The formulation is sufficiently general that P_d may vary by a power of ten, while the pore geometry constant remains nearly unchanged (i.e. the size of the grains spans a range of values but

the curvature of the Pc curve remains similar): **Figure 14.**

In practice, we typically express one variable as a function of the other (rather than the product being a constant), and so **the relation is written as below.**

$$[\text{Log}(V_b / V_{b_\infty})] = \text{Constant} / [\text{Log}(P_c / P_d)]$$

One proceeds to a direct (non-logarithmic) expression for V_b / V_{b_∞} by raising each side of the equation to the power 10, Figure 13 per George Hirasaki, and then introducing the Natural Logarithm/Exponential.

$$V_b / V_{b_\infty} = 10^{\{\text{Constant}/[\text{Log}(P_c / P_d)]\}}$$

The Thomeer Capillary Pressure Model

•**Thomeer's model is surprisingly robust. Consider the case of relatively well sorted samples with similar porosities but different grain sizes.**

- As grain size drops we anticipate a decrease in perm and an increase in displacement pressure.
- It is an underlying relation between displacement pressure and permeability/grain-crystal size that forms the basis for Lucia's classification protocol.
- Although P_d varies by an order of magnitude there is little change in the pore geometrical parameter.
- Notice that V_{b_∞} is close to the porosity, ϕ , for the highest perm sample but can be significantly less for lower perm samples.

George Hirasaki. Hydrostatic Fluid Distribution. www.owlnet.rice.edu/~ceng671/CHAP3.pdf

Curve	ϕ	k_{rel} , md	$(V_b)_\infty$	P_d	G
A	0.216	430	0.215	6.7	0.2
B	0.220	116	0.15	16	0.1
C	0.196	13.4	0.145	26	0.2
D	0.197	1.2	0.135	65	0.2

Mercury/air capillary pressure curves (Jordan and Campbell, 1984), from Hirasaki.

Figure 14

See Appendix 1 for details of following conversion to exponential form.

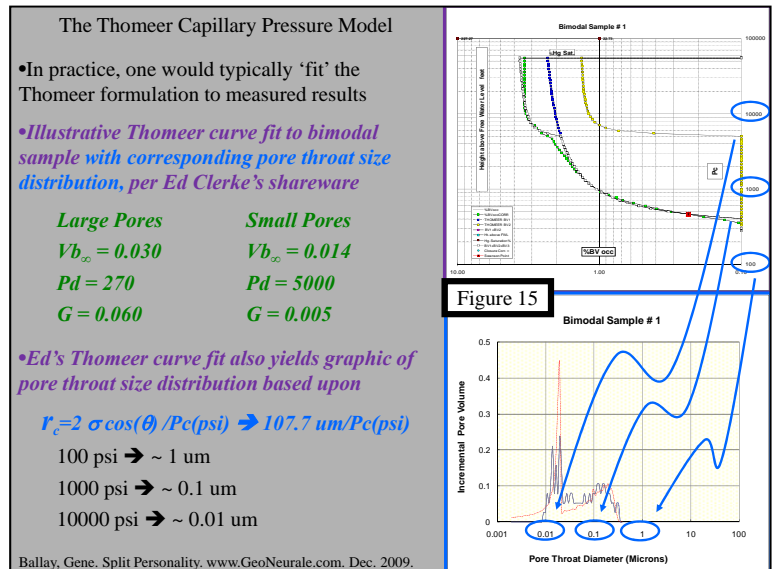
$$V_b / V_{b\infty} = 10^{\{ \text{Constant} / [\text{Log}(P_c / P_d)] \}} \rightarrow \exp[-G / \text{Log}(P_c / P_d)]$$

$$- G = 0.4343 * \text{Constant}$$

Both common and natural logarithms are being referenced, **Base 10 and Base e. When drawing upon someone else's curve fit parameters, or performing our own, we must follow a consistent use of the two logarithmic bases.**

Although **the Thomeer protocol was widely used within Shell** (where Thomeer worked), it was **less commonly seen outside Shell**. Never-the-less, it **has a number of conceptual and practical attractions relative to the Square Root (Perm/Porosity) and Flow Zone Indicator (FZI) alternatives**: Appendix 2.

In the case of multiple pore size distributions, for example, **the individual Thomeer representations can be super-imposed** to mathematically represent the composite response: **Figure 15.**



Although the laboratory measurements report Pressure, a more physically meaningful attribute is the radius (or diameter) of the pore throat size that is being penetrated at that particular pressure. In the case of mercury injection data the two are related as follows.

$$P_c = 2 \sigma \cos(\theta) / r_c$$

$$r_c(\text{microns}) = 107.7 \text{ um} / P_c(\text{psi})$$

Thinking of the response in terms of pore throat size is akin to thinking in terms of pore body size and/or grain/crystal size, which is an underlying basis for the Lucia carbonate classification protocol.

From **a somewhat different perspective, Dale Winland and Ed Pittman examined correlations of porosity, permeability and capillary pressure curves to recognize an optimal relation against r35**, the pore throat radius being touched by the non-wetting mercury at 35% saturation.

As discussed in detail by Hartmann, r35 breaks the Phi-Perm crossplot into domains similar to (the perhaps more common) Permeability/Porosity ratio, but has the attraction of being a physically meaningful attribute; the pore throat radius being touched when the non-wetting phase saturation is 35%.

r35 is directly related to the corresponding mercury injection pressure, and can also be used as a generic rock quality indicator.

It's worth explicitly pointing out that, particularly in the case of legacy data, the Pc measurements may not have been made at reservoir conditions (Mitchell, 2003) and one should be alert for the implications.

Dual Porosity in the Water Leg

We shall **focus on the simplest configuration, a double porosity system with the two base elements arranged in parallel**: **Figure 16**. This is the conceptual equivalent of Diederix, Swanson, Fleury and others and will serve to illustrate the issue.

The spreadsheet is designed to construct the Thomeer Pc curve for a double porosity system, with each element specified (displacement pressure, porosity, pore geometry factor) by the User, **thereby allowing locally specific applications**.

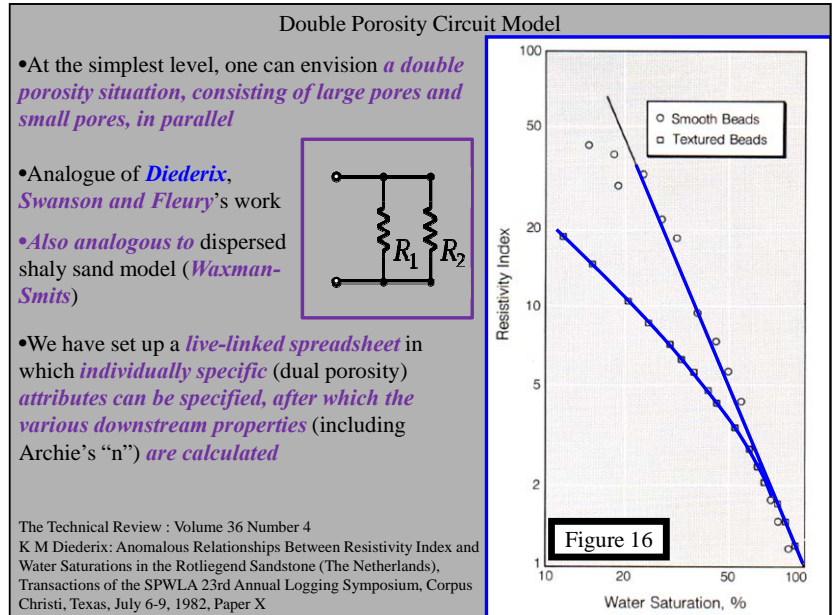
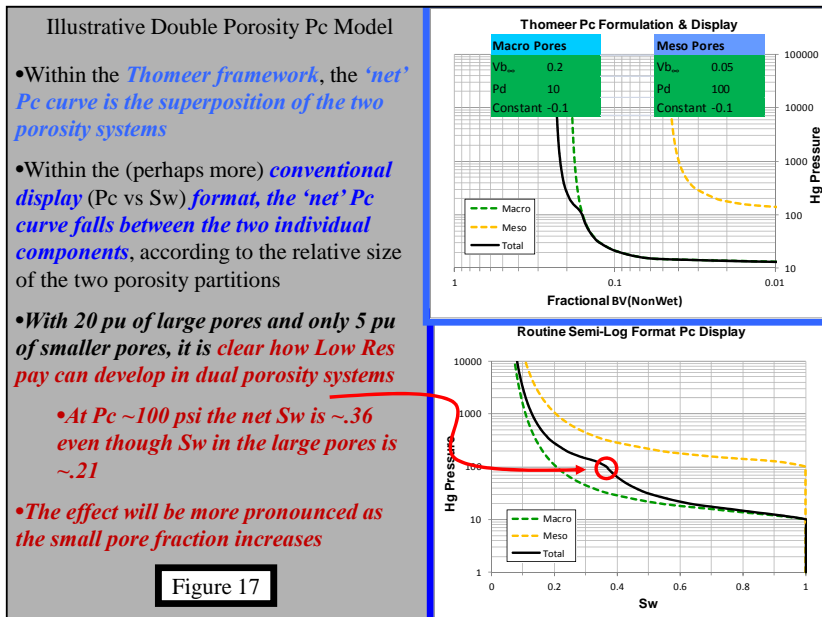
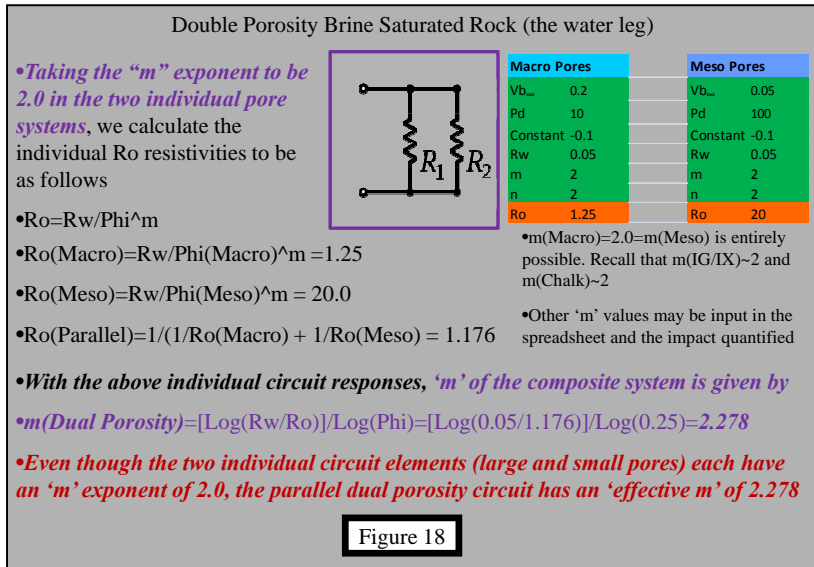


Figure 17 is an illustrative example, in which the total porosity consists of 20 pu of large pores and 5 pu of small pores. Each system has its unique capillary response, and the composite response falls between these two boundaries according to the porosity partition (relative populations of large and small pores).



Each system has its unique capillary response, and the composite response falls between these two boundaries according to the porosity partition (relative populations of large and small pores).

With only 20 % of the pore system being small (i.e. 5 pu of a total 25 pu), it becomes immediately clear how Low Res pay can develop in a double porosity pore system.

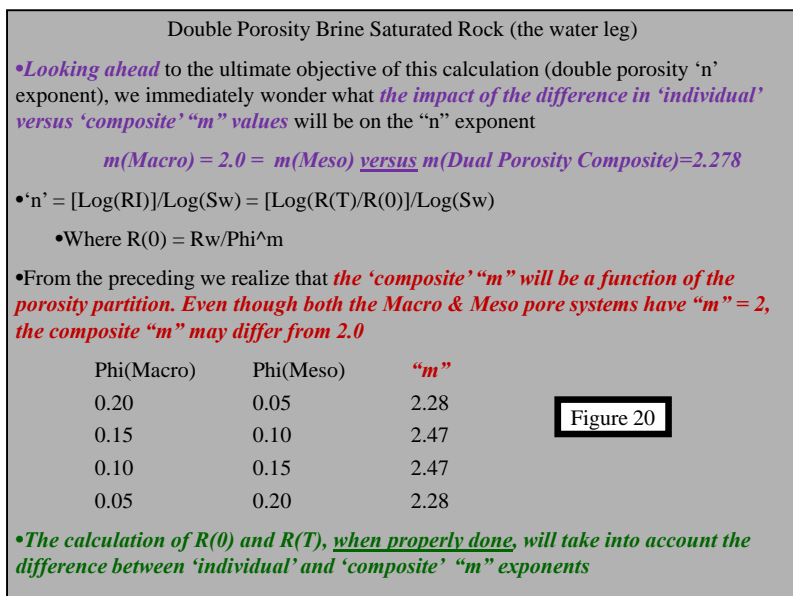
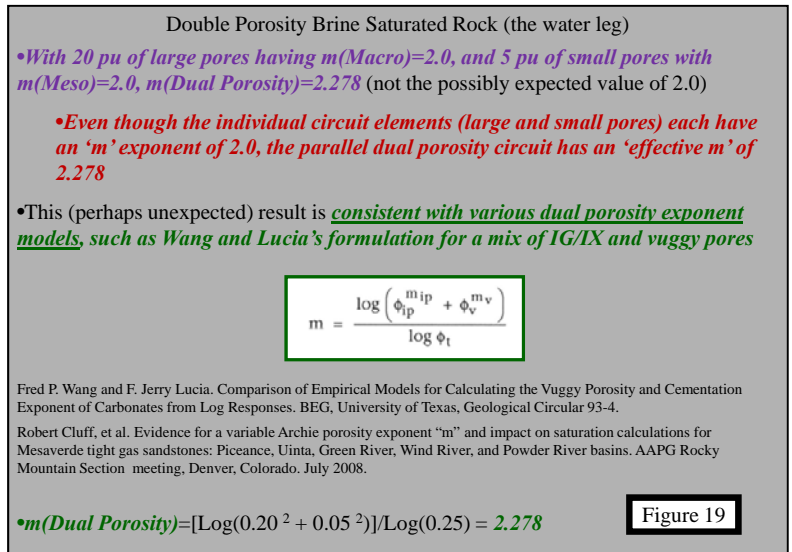


As discussed in our earlier note (Archie’s “m” Exponent) the pore system and cementation exponent have an intuitively obvious relation. Perhaps *less intuitive is the fact that if both elements (large and small pores) in a parallel circuit have an “m” of 2.0 (IG/IX and chalk may both have “m”~2.0), the “net m” of the reservoir rock is not 2.0, but rather related to the relative proportions of*

the two components: Figure 18.

This observation is not new, and has been reported by Wang & Lucia, Cluff, and others: Figure 19.

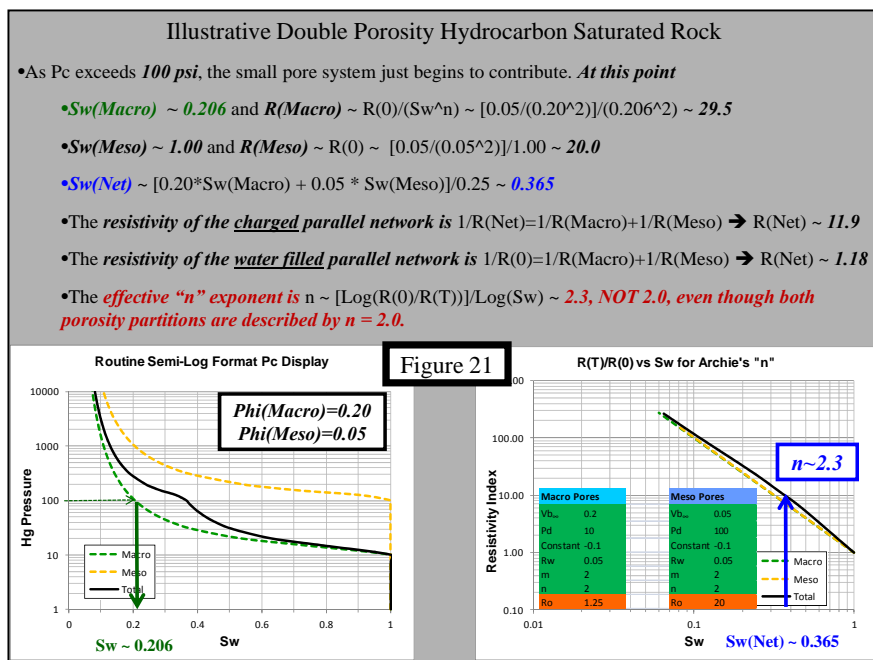
Looking ahead to our “n” objective, we may recognize the “m” dependence by either calculating it according to the elementary circuit responses (which is what we have done), or with a double porosity model such as Wang & Lucia: Figure 20.



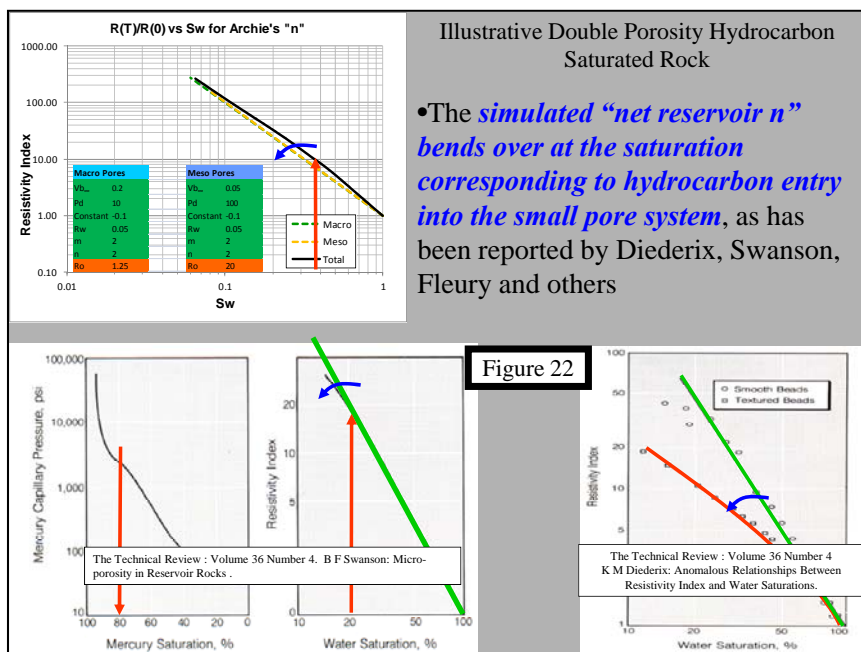
Dual Porosity in the Hydrocarbon Column

With an understanding of the basic circuit theory, the capillary pressure curve and the water leg response, we are ready to (simply) simulate the effect of a dual porosity system on the “n” exponent: Figure 21.

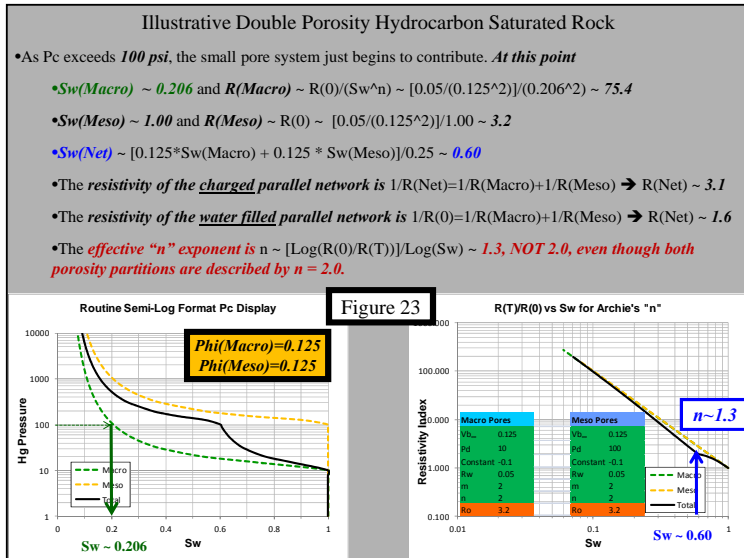
With the illustrative parameters, hydrocarbon does not enter the small pores at mercury pressures lower than 100 psi. As the hydrocarbon begins to enter the small pores there is already a significant penetration into the large pores, with the relative and net saturations as seen in Figure 21.



The two volumetric distributions (at each and every pressure) and the assumption of a parallel network, allow calculation of the “n” exponent. **What we find, perhaps unexpectedly** but

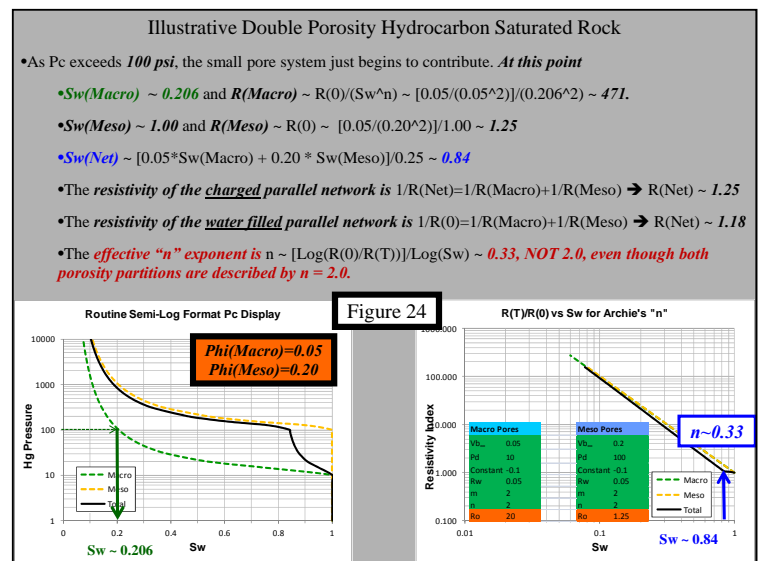


somewhat analogous to the earlier discussion of dual porosity “m” exponents, **is that even though the two individual systems have an “n” of 2.0 (quite possible, with for example a mix of IG/IX and Chalk), the “effective n” of the system is not 2.0 but rather something higher, and it “bends over” at the bulk saturation corresponding to entry of the non-wetting phase into the smaller pores: Figure 22.**



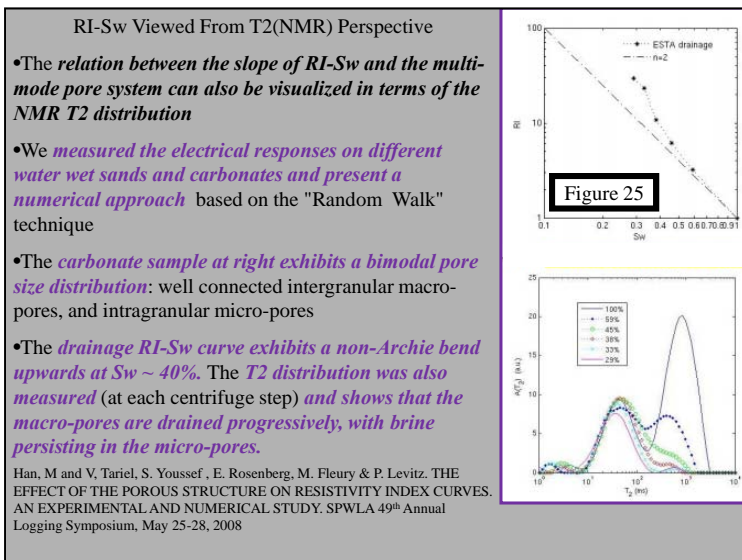
RI-Sw crossplot “bends upwards” when hydrocarbon penetrates the small pore system.

For completeness, we have taken the calculation to the “small pore dominated configuration”, **Figure 24**. The hydrocarbon easily enters the large pores, but they are only a small portion of the total pore system, and the effect noted in Figure 23 is even more pronounced.



The calculations herein are based upon a Pc-driven RI-Sw simulation. **Fleury offers another perspective, that of T2(NMR) and RI-Sw: Figure 25.**

Again, one finds that in a double porosity system, not only can the “m” exponent be affected, but so too can Archie’s “n”.



Summary

While there is an intuitive connection between Archie's cementation exponent and pore geometry, it is less obvious to expect the basic pore system to also affect "n".

Given that "n" represents the relative conductive efficiency of the hydrocarbon saturated rock and brine saturated rock, wettability is immediately recognized as affecting "n".

We have set the wettability issue aside for the moment (assigned "n" = 2.0 to both pore systems, which is one of several possibilities) and used capillary pressure volumetrics to populate two circuit elements (large and small pores, assumed to be in a parallel configuration), which then allows one to calculate the "effective n" of the double porosity system.

The parallel circuit assumption is common in the literature and analogous to how dispersed shaly sands are evaluated. One must bear in mind, however, that Nature does not always assume a mathematically convenient configuration.

The calculation is accomplished with a dynamic spreadsheet that coordinates the Pc and RI-Sw responses, and allows User specified (locally appropriate) pore distribution attributes.

In practice, were one to have an actual Pc data base of interest, Excel's Solver feature could be used to determine the corresponding Thomeer Pc parameters and a simulation of "n" then performed.

While admittedly simple, the result is found to reproduce the behavior observed by Diederix, Swanson, Fleury and others, and offers the attraction of:

- 1) explicitly links Pc and RI-Sw in both digital and graphical format,
- 2) can accommodate locally specific attributes for first pass "what if" determinations.

Acknowledgements

We appreciate Marc Fleury generously taking the time to compare our spreadsheet results to his MatLab model, to ensure consistency.

Mohamed Efnik, Miguel Exposito, Michel Krief and Martin Storey graciously provided us with detailed review and commentary.

Appendix 1: Logarithms

In today's computerized world, the utility of logarithms may not be immediately obvious, but in their time they constituted a 'giant step forward' in a manner somewhat similar to the hand calculators and laptop computers in use today.

Logarithms can be defined with respect to any positive base, and will differ one base to the next by only a constant multiplier. Since our calculations are usually in a Base 10 number system (we

have ten fingers and ten toes, and the human mind built upon that), that reference is one obvious choice.

Log10(x) is defined as is the power to which 10 must be raised, in order to yield the value x.

- Log10(1) = 0, since 10⁽⁰⁾=1
- Log10(10) = 1, since 10⁽¹⁾=10
- Log10(100) = 2, since 10⁽²⁾=100

Another *natural base* arises within the context of calculus, as the area under the curve f(x) = 1/x, from 1 → x. Now the base (reference) is the irrational number e ≈ 2.718281828.

The utility of logarithms lies in the fact that multiplication of actual numbers is accomplished by addition of logarithms, and division of actual numbers corresponds to subtraction of their logarithms. One is then able to perform calculations much quicker, and with less chance of error.

Next, recognizing that multiplication is achieved with addition, we realize that by scaling two linear objects in an appropriate manner, multiplication may be done by adding the respective, appropriate lengths of the two numbers in question: the slide rule. The slide rule of yesterday is the analogue of the hand calculator of today.

In addition to simplifying multiplication and subtraction, logarithms are also attractive when dealing with equations that involve an exponential term, such as radioactive decay, etc and it is in this context (and others) that natural (Base e) logarithms become attractive: hence the characterization of this base as ‘natural’.

Base 10 and Base e logarithms differ only by a constant multiplier.

Number	Log10(x)	Ln(x)	Ratio
1	0	0	Log(x)/Ln(x)
10	1	2.302585	0.43429448
100	2	4.60517	0.43429448
1000	3	6.907755	0.43429448

In the case at hand, the relation of interest is

$$Vb / Vb_{\infty} = 10^{\{ \text{Constant} / [\text{Log}(Pc / Pd)] \}} \rightarrow \exp[-G / \text{Log}(Pc / Pd)]$$

The conversion to Base e follows

$$[\text{Log}(Vb / Vb_{\infty})] = \text{Constant} / [\text{Log}(Pc / Pd)]$$

$$\text{Log}(Vb / Vb_{\infty}) = (1/0.4343)[\text{Ln}(Vb / Vb_{\infty})]$$

$$\text{Ln}(Vb / Vb_{\infty}) = 0.4343\{\text{Constant} / [\text{Log}(Pc / Pd)]\}$$

$$(Vb / Vb_{\infty}) = \exp\{0.4343\{\text{Constant} / [\text{Log}(Pc / Pd)]\}\} = \exp[-G / \text{Log}(Pc / Pd)]$$

$$\Rightarrow -G = 0.4343 * \text{Constant}$$

Appendix 2: Properties of Thomeer Hyperbolae

Courtesy Ed Clerke

- A single pore system can be represented by one Thomeer hyperbolae and is completely characterized by just three numbers; P_d , $B_{v,\infty}$, G .
- The Thomeer hyperbolae rely upon no other attributes (with associated errors and uncertainties); it is self-contained.
- A Petrophysical Rock Type (PRT) can be defined as a cluster in Thomeer parameter space; P_d , $B_{v,\infty}$, G .
- Air permeability can be computed and predicted from the pore network parameters, P_d , $B_{v,\infty}$, G , to within a multiplicative uncertainty of 1.8x, and this can be compared to a measured permeability (as a Quality Control device).
- The Thomeer hyperbolae obey the law of superposition and can then be combined (superposed) to quantify complex pore systems.
- A Thomeer forward modeled capillary pressure curve can be generated from insight into the attributes which may come from a variety of sources of rock data; cores to cuttings to a Rock Catalog.

References

- Abdallah, Wael et al. Fundamentals of Wettability. Oilfield Review. Summer 2007.
- Alsayari, Saif et al. THE INFLUENCE OF WETTABILITY ON PETROPHYSICAL PROPERTIES. SCA2009-42.
- Archie, G. E. The Electrical Resistivity Log as an Aid in Determining Some Reservoir Characteristics, Petroleum Transactions of the AIME 146 (1942): 54-62.
- Archie, G. E. Electrical Resistivity: An Aid In Core Analysis Interpretation. AAPG Vol 31 No 2 (1947).
- Archie, G. E. Classification of Carbonate Reservoir Rocks and Petrophysical Considerations, AAPG Bulletin Vol 36 No 2 (1952): 278 - 296
- Ballay, Gene. Split Personality. www.GeoNeurale.com. Dec. 2009.
- Ballay, Gene. The “m” Exponent in Carbonate Petrophysics. www.GeoNeurale.com. Jan. 2012.
- Bauer, D. et al. From computed microtomography images to resistivity index calculations of heterogeneous carbonates using a dual-porosity pore-network approach: Influence of percolation on the electrical transport properties. Physical Review. 2011.
- Bouvier, Lucienne et al. Reconciliation of Log and Laboratory Derived Irreducible Water Saturations in a Double Porosity Reservoir. Publication details n/a; found with Google.
- Clerke, Edward and Harry W Mueller, Eugene C Phillips, Ramsin Y Eyvazzadeh, David H Jones, Raghu Ramamoorthy & Ashok Srisvastava. Application of Thomeer Hyperbolas to decode the

pore systems, facies and reservoir properties of the Upper Jurassic Arab D Limestone, Ghawar Field, Saudi Arabia: A "Rosetta Stone" approach. *GeoArabia*, Vol 13 No 4 2008.

Clerke, Ed. Permeability, Relative Permeability, Microscopic Displacement Efficiency and Pore Geometry of M₁ Bimodal Pore Systems in Arab D Limestone. SPE Middle East Oil and Gas Show. Bahrain. March 2007.

Clerke, Ed. Beyond Porosity-Permeability Relationships-Determining Pore Network Parameters for the Ghawar Arab-D Using the Thomeer Method. 6th Middle East Geoscience Conference. Bahrain. March, 2004.

Clerke, E.A. and P.R. Martin 2004. Thomeer Swanson Excel spreadsheet: FAQ's and user comments. Presented and distributed at the SPWLA 2004 Carbonate Workshop, Noordwijk.

Cluff, Robert et al. Evidence for a variable Archie porosity exponent "m" and impact on saturation calculations for Mesaverde tight gas sandstones: Piceance, Uinta, Green River, Wind River, and Powder River basins. AAPG Rocky Mountain Section meeting, Denver, Colorado. July 2008.

Crain, Ross. Myth : High Water Saturation Means Water Production. www.spec2000.net. 2009.

Diederix, K. M. Anomalous Relationships Between Resistivity Index and Water Saturations in the Rotliegend Sandstone (The Netherlands), Transactions of the SPWLA 23rd Annual Logging Symposium, Corpus Christi, Texas, July 6-9, 1982, Paper X

Efnik, M. S. et al. Evaluation of Water Saturation from Laboratory to Logs. SCA2006-56.

Glover, Paul. A generalized Archie's law for n phases. *GEOPHYSICS*, VOL. 75, NO. 6, NOVEMBER-DECEMBER 2010; P. E247-E265.

Glover, Paul. What is the saturation exponent? A new interpretation. Publication details n/a, found with Google.

Fleury, Marc. Resistivity in Carbonates: New Insights. SCA 2002-28.

Fleury, Marc et al. Evaluation of water saturation from resistivity in a carbonate field. From laboratory to logs. SCA 2004.

Grader, A. et al. A COMPARATIVE STUDY OF DIGITAL ROCK PHYSICS AND LABORATORY SCAL EVALUATIONS OF CARBONATE CORES. SCA2010 Paper A012.

Han, M. et al. The effect of the pore structure on resistivity index curves. International Symposium of the Society of Core Analysts held in Calgary, Canada, September, 2007.

Han, M. et al. Deviation from Archie law in partially saturated porous media: wetting film versus disconnectedness of the conducting phase. Journal details n/a.

Hartmann, Dan and Edward Beaumont. Predicting Reservoir System Quality and Performance.

www.searchanddiscovery.net/documents/beamont/index.htm

Hirasaki, George. Hydrostatic Fluid Distribution.

www.ruf.rice.edu/~che/people/faculty/hirasaki/hirasaki.html

Transport Phenomena

www.owl.net.rice.edu/~chbe402/

Flow & Transport in Porous Media I. Geology, Chemistry and Physics of Fluid Transports

www.owl.net.rice.edu/~ceng571/

Flow & Transport in Porous Media II. Multidimensional Displacement

www.owl.net.rice.edu/~chbe671/

Kanu, M. O. et al. Effect of Electrical Resistivity Measurement on Archie's Saturation Exponent. World Journal of Applied Science and Technology, Vol.3. No.1 (2011).

Keller, G. V. Effect of Wettability on the Electrical Resistivity of Sand, Oil & Gas Journal 51 (January 5, 1953): 62-65.

Lasswell, Patrick. LABORATORY ANALYSIS OF ELECTRICAL ROCK PROPERTIES AND CAPILLARY PRESSURE IN FULL DIAMETER CORE SAMPLES. SCA2005-75.

Li, Kewen. DETERMINATION OF RESISTIVITY INDEX, CAPILLARY PRESSURE, AND RELATIVE PERMEABILITY. PROCEEDINGS, Thirty-Fifth Workshop on Geothermal Reservoir Engineering Stanford University, Stanford, California, February 1-3, 2010

Li, Kewen et al. RELATIONSHIP BETWEEN CAPILLARY PRESSURE AND RESISTIVITY INDEX. SCA2005-14.

Lucia, Jerry. The Oilfield Review. Winter 2000.

Lucia, Jerry. Rock Fabric/Petrophysical Classification of Carbonate Pore Space for Reservoir Characterization. AAPG Bulletin 79, no. 9 (September 1995): 1275-1300.

Lucia, Jerry. Petrophysical parameters estimated from visual description of carbonate rocks: a field classification of carbonate pore space. Journal of Petroleum Technology. March, v. 35, p. 626-637. 1983.

Lucia, Jerry. www.beg.utexas.edu

Masalmeh, S. K. et al. Improved Characterization and Modeling of Capillary Transition Zones in Carbonate Reservoirs. SPE Reservoir Evaluation & Engineering. April 2007.

Mitchell, P., Sincock, K. and Williams, J.: "On the Effect of Reservoir Confining Stress on Mercury Intrusion-Derived Pore Frequency Distribution," Society of Core Analysis, SCA 2003-23.

Montaron, Bernard. Connectivity Theory – A New Approach to Modeling Non-Archie Rocks. SPWLA 49th Annual Logging Symposium, May 25-28, 2008

Phillips, E. C., Clerke, E. A., Buiting, J. M., (2009), Full Pore System Petrophysical Characterization Technology for Complex Carbonates – Results from Saudi Arabia, AAPG Annual Conference, Denver, June.

Potocki, Dan et al. CARBONATE ROCK WETTABILITY INTERPRETED FROM CAPILLARY PRESSURE AND IMBIBITION RESISTIVITY INDEX ANALYSES. SCA2003-03.

Schlumberger Technical Review. Volume 36 Number 3.

Schlumberger Technical Review. Volume 36 Number 4.

Suman, Ravi et al. Effects of pore structure and wettability on the electrical resistivity of partially saturated rocks – A network study. *GEOPHYSICS*, VOL. 62, NO. 4 (JULY-AUGUST 1997); P. 1151–1162,

Swanson, B. F. Microporosity in Reservoir Rocks - Its Measurement and Influence on Electrical Resistivity, Transactions of the SPWLA 26th Annual Logging Symposium, Dallas, June 17-20, 1985, paper H.

Sweeney, S. A. and H Y Jennings Jr: The Electrical Resistivity of Preferentially Water-Wet and Preferentially Oil-Wet Carbonate Rock, *Producers Monthly* 24, No 7 (May 1960): 29-32

Thomeer, J.H.M., Introduction of a Pore Geometrical Factor Defined by a Capillary Pressure Curve, *Petroleum Transactions, AIME*, Vol 219, 1960.

Thomeer, J.H.M. Air Permeability as a Function of Three Pore-Network Parameters, *Journal of Petroleum Technology*, April, 1983.

Toumelin, E. and C. Torres-Verdín. Influence of Oil Saturation and Wettability on Rock Resistivity Measurements: A Uniform Pore-Scale Approach. Annual SPWLA Logging Symposium, June, 2005.

Toumelin, E. Pore-Scale Petrophysical Models for the Simulation and Combined Interpretation of Nuclear Magnetic Resonance and Wide-Band Electromagnetic Measurements of Saturated Rocks. PhD Dissertation. University of Texas, Austin.

Watfa, M. Using Electrical Logs to Obtain the Saturation Exponent (n) in the Archie Equation. SPE Middle East Oil Show. Bahrain. November 1991.

Wang, Fred P. and F. Jerry Lucia. Comparison of Empirical Models for Calculating the Vuggy Porosity and Cementation Exponent of Carbonates from Log Responses. BEG, University of Texas, Geological Circular 93-4.

Wyllie, M. R. and A. R. Gregory: Formation Factors of Unconsolidated Porous Media: Influence of Particle Shape and Effect of Cementation, *Petroleum Trans of the AIME* (1953): 103-110.

Youssef, S. et al. High Resolution u-CT Combined to Numerical Models to Assess Electrical Properties of Bimodal Carbonates. SCA2008-37.

Yue, Wenzheng et al. Numerical Experiments of Pore Scale for Electrical Properties of Saturated Digital Rock. *International Journal of Geosciences*, 2011, 2, 148-154.

Biography

R. E. (Gene) Ballay's 35 years (18 homes, 14 countries) in petrophysics includes both research and operations assignments with carbonate experience ranging from individual Niagaran reefs in Michigan to the Lisburne in Alaska through Ghawar, Saudi Arabia (the largest oilfield in the world).

He holds a PhD in Theoretical Physics with double minors in Electrical Engineering & Mathematics, has taught physics in two universities, mentored Nationals in Indonesia and Saudi Arabia, published numerous technical articles and been designated co-inventor on both American and European patents.

At retirement from the Saudi Arabian Oil Company he was the senior technical petrophysicist in the Reservoir Description Division and had represented petrophysics in three multi-discipline teams, each bringing on-line multi-billion barrel increments.

Subsequent to retirement from Saudi Aramco he established Robert E Ballay LLC, which provided physics - petrophysics consulting services.

He served in the US Army as a Microwave Repairman and in the US Navy as an Electronics Technician: he is a USPA Parachutist, a PADI nitrox certified Dive Master and a Life Member of Disabled American Veterans.

This article brings to a close his career, and he bids a fond farewell to the many colleagues with whom he has worked.



Nelson Suarez Arcano is a Petrophysicist with 7 years of experience in operations and asset studies, presently working carbonates for Dubai Petroleum Establishment.

He began his career in the always interesting unconsolidated extra-heavy / heavy oil sands of the Orinoco Belt in Venezuela (SINCOR C.A), where he also mentored newly graduated Engineers and Geologists. Following Venezuela, he worked for Paradigm in United Arab Emirates, Oman, Kuwait, Qatar, Saudi Arabia and India.



He holds a BS (Cum Laude) in Petroleum Engineering from Universidad De Oriente – Nucleo Anzoategui (Venezuela) where he taught “Petrophysical Logs” as Associate Professor, and is presently enrolled in an MS (Petroleum Engineering) program with Heriot-Watt University.